Physica 12D (1984) 3–18
North-Holland, Amsterdam

1.1. LIQUIDS

AN OVERVIEW OF RAYLEIGH–TAYLOR INSTABILITY*

D.H. SHARP
Theoretical Division, Los Alamos National Laboratory, Los Alamos, New Mexico 87545, USA

The aim of this talk is to survey Rayleigh–Taylor instability, describing the phenomenology that occurs at a Taylor unstable interface, and reviewing attempts to understand these phenomena quantitatively.

1. Introduction

The Rayleigh–Taylor instability is a fingering instability of an interface between two fluids of different densities, which occurs when the light fluid is pushing the heavy fluid [1, 2]. The aim of this talk is to survey Rayleigh–Taylor instability, describing the phenomenology that occurs at a Taylor unstable interface, and reviewing attempts to understand these phenomena quantitatively. I will also emphasize some critical questions which require further study.

2. Simplest explanation of the occurrence of Rayleigh–Taylor instability

This conference affords the pleasure of learning about a great variety of topics from speakers with the most diverse backgrounds. In view of this diversity, I hope the experts will forgive me if I begin with the simplest possible description of Rayleigh–Taylor instability.

Imagine the ceiling of a room plastered uniformly with water to a depth of 1 meter (fig. 1). The layer of water will fall. However, it is not through lack of support from the air that the water will fall. The pressure of the atmosphere is equivalent to that of a column of water 10 meters thick, quite sufficient to hold the water against the ceiling. But in one respect the atmosphere fails as a supporting medium. It fails to constrain the air–water interface to flatness. No matter how carefully the water layer was prepared to begin with, it will deviate from planarity by some small amount. Those portions of the fluid which lie higher than the average experience more pressure than is needed for their support. They begin to rise, pushing aside water as they do so. A neighboring portion of the fluid, where the surface hangs a little lower than average, will require more than average pressure

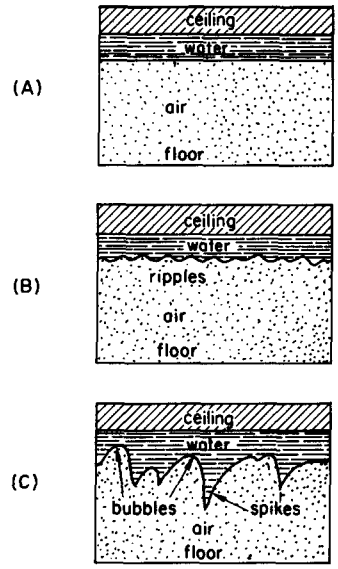

Fig. 1. (A) The pressure of the air is quite sufficient to support a perfectly uniform layer of water 1 meter thick against the ceiling. (B) But the air pressure can not constrain the air–water interface to flatness. Ripples or irregularities will inevitably be present at the interface. (C) The irregularities grow, forming "bubbles" and "spikes." The water falls to the floor.

* Work supported by the U.S. Department of Energy.

for its support. It begins to fall. The air cannot supply the variations in pressure from place to place necessary to prevent the interface irregularities from growing. The initial irregularities therefore increase in magnitude, exponentially with time at the beginning. The water which is moving downward concentrates in spikes. The air moves upward through the water in round topped columns. The water falls to the floor.

The same layer of water lying on the floor would have been perfectly stable. Irregularities die out. Thus we can infer a simple criterion for the onset of Taylor instability at the interface between two fluids of different densities: *If the heavy fluid pushes the light fluid, the interface is stable. If the light fluid pushes the heavy fluid, the interface is unstable.* A criterion of comparable simplicity governs the onset of Kelvin–Helmholtz instability: *The interface between two fluids is unstable if there is a jump in the tangential component of the velocity across the interface.* These two criteria are among the most basic principles in the subject of interface instability.

3. Examples of Rayleigh–Taylor instability

Taylor instability occurs in diverse situations. As examples, we mention:

A. *Natural phenomena*

i) Overturn of the outer portion of the collapsed core of a massive star [3];

ii) the formation of high luminosity twin-exhaust jets in rotating gas clouds in an external gravitational potential [4].

B. *Technological applications*

i) Laser implosion of deuterium–tritium fusion targets [5];

ii) electromagnetic implosion of a metal liner [6], and several others.

Let us take a quick look at one of these examples. A highly schematic picture of the implosion of a deuterium–tritium (DT) pellet is as follows (fig. 2). A sphere of DT is surrounded by a glass or metal tamper. This tamper is irradiated with intense laser light, which causes it to accelerate inward. The outer surface of the tamper is the interface between a heavy fluid (metal) and a light fluid (vaporized metal) and is unstable during the initial phase of the implosion. As the pellet is compressed to perhaps 1,000 times its normal density, its pressure increases until it is sufficient to slow the inward motion of the tamper. This phase of the implosion is also Taylor unstable; here it is the DT which is pushing the tamper. Although this picture of the implosion of a DT pellet is so oversimplified as to be almost ridiculous, it nevertheless suggests quite clearly that Taylor instability is a factor to be dealt with in evaluating pellet performance [7].

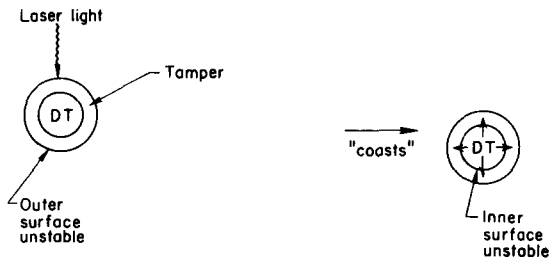

Fig. 2. Schematic diagram of the implosion of DT pellet.

4. Phenomenology of Rayleigh–Taylor instability

There is a complex phenomenology associated with the evolution of a Taylor unstable interface. This includes the formation of spikes, curtains and bubbles, the development of Helmholtz instability on the side of the spikes, competition among bubbles leading to their amalgamation, formation of droplets, entrainment and turbulent mixing, and a possible chaotic limit with a fractalized interface.

It is helpful to organize a description of the growth of the instability into a number of stages. This can be done as follows [8, 9].

Stage 1. If the initial perturbations in the interface or velocity field are extremely small, the early stages in the growth of the instability can be analyzed using the linearized form of the dynam-

ical equations for the fluid. The result is that small amplitude perturbations of wavelength λ grow exponentially with time. When the amplitude of the initial perturbation grows to a size of order 0.1λ to 0.4λ, substantial deviations from the linear theory are observed.

Stage 2. During the second stage, while the amplitude of the perturbation grows nonlinearly to a size of order λ, the development is strongly influenced by three-dimensional effects and the value of the density ratio, or Atwood number $A = (\rho_H - \rho_L)/(\rho_H + \rho_L)$, where ρ_H = density of heavy fluid, ρ_L = density of light fluid.

If $A \lesssim 1$, the light fluid moves into the heavy fluid in the form of round topped bubbles with circular cross sections. Note that "two-dimensional" plane bubbles are unstable to perturbations along the axis perpendicular to the plane of the bubble, and a trough having a plane bubble as a cross section will break up into three-dimensional bubbles. The heavy fluid will form spikes and walls or curtains between the bubbles, so that a horizontal section would show a honeycomb pattern. If $A \gtrsim 0$, one will instead find a pattern more like two sets of interpenetrating bubbles.

Note that these pictures are rather different from the simpler patterns of bubbles and spikes that we think of in two dimensions. I will nevertheless often refer to bubbles and spikes for the sake of simplicity.

Stage 3. The next stage is characterized by the development of structure on the spikes and interactions among the bubbles. These phenomena can originate from several sources. There is a nonlinear interaction among initial perturbations of different frequency. Also Helmholtz instability along the side of the spike can cause it to mushroom, increasing the effect of drag forces on the spike. This effect is more pronounced at low density ratios. There is some experimental evidence for bubble amalgamation, a process in which large bubbles absorb smaller ones, with the result that large bubbles grow larger and move faster.

The presence of heterogeneities in various physical quantities can modify the shape and speed of bubbles and spikes to a degree which depends on the strength and length scale of the heterogeneity.

Stage 4. In the final stage, we encounter the breakup of the spike by various mechanisms, the penetration of a bubble through a slab of fluid of finite thickness and other complicated behavior

Table I
Some factors influencing the development of Rayleigh–Taylor instability

Factor	Relative size of effect (dimensionless parameter)	Effect on growth of instability
Density ratio	ρ_H/ρ_L or $A = (\rho_H - \rho_L)/(\rho_H + \rho_L)$	A key factor governing the growth rate of Rayleigh–Taylor or Kelvin–Helmholtz instability for small amplitude perturbations of wavelength λ.
Surface tension	Weber number $= 2\sigma/(\rho_H - \rho_L)g\lambda^2$	In linear theory, stabilizes wavelengths shorter than a critical wavelength $\lambda = \sqrt{\sigma/g(\rho_H - \rho_L)}$. Establishes a most unstable wavelength, hence probably makes problem well posed mathematically.
Viscosity	$R = vt/\lambda^2$	Reduces growth rate; regularizes fluid flow.
Compressibility	$G = g/kc^2 = \dfrac{(\text{phase velocity of gravity waves})^2}{(\text{sound speed})^2}$	Reduces growth rate of long wavelength perturbations; decreases active volume of fluid.
Heterogeneity	$\Delta L/\lambda$, $\Delta v/v \ldots$	Can excite secondary, tertiary, ... instabilities of various wavelengths.

that leads to a regime of turbulent or chaotic mixing of the two fluids.

5. Factors influencing the development of Rayleigh–Taylor instability

Numerous factors influence the development of Taylor instability in a simple fluid. These include surface tension, viscosity, compressibility, effects of converging geometry, three-dimensional effects, the time dependence of the driving acceleration, shocks, and a variety of forms of heterogeneity. An assessment of some of these factors is given in table I.

6. Other factors which may be operative in realistic problems

In natural phenomena and technological applications where Taylor instability occurs, there are many other factors that can play an important role. For example, material properties and the equation of state of the fluids may be important. The fluids may conduct heat or diffuse mass. The material may change phase or consist of several components. Radiation often couples to hydrodynamics.

It is not easy for me to imagine dealing scientifically with the whole range of factors that can influence Rayleigh–Taylor instability, so in this talk I will restrict myself to a few of the factors which effect the behavior of simple fluids. It is a little bit humbling to recall that engineers must deal with Taylor instability in its full complexity.

7. Analytic and quasi-analytic modeling

The purpose of analytic modeling is to identify the effects which are dominant during a given stage in the development of the instability.

7.1. *Linear analysis*

There is a considerable body of literature which analyzes the initial stage in the growth of small amplitude Taylor instability, where the linearized form of the equations of fluid dynamics can be used.

7.1.1. *Plane geometry*

As an example, consider two infinitely extended inviscid fluids which meet at a plane interface (fig. 3). For definiteness, we suppose the upper fluid is heavier, $\rho_H > \rho_L$. The fluids are subjected to a constant acceleration in a direction normal to the interface. We write the total effective acceleration as $\boldsymbol{G} = (\boldsymbol{a} - \boldsymbol{g}) = (a + g)\hat{z} = G\hat{z}$, with $g > 0$ and $\hat{z}$ a unit vector normal to the interface, pointing into the heavy fluid. The gravitational acceleration is $\boldsymbol{g} = -g\hat{z}$ and $\boldsymbol{a} = a\hat{z}$ is a uniform external acceleration applied to the system as a whole. Thus, when $G > 0$, the effective acceleration acts vertically upward, the light fluid accelerates the heavy fluid, and the configuration is unstable according to the criterion we discussed above.

One works in a noninertial frame comoving with the unperturbed interface. In this frame, the unperturbed fluids are at rest and the unperturbed interface is defined by $z = 0$. The pressure fields in the fluids vary with the vertical coordinate z to balance the total acceleration and permit static equilibrium (in the comoving frame).

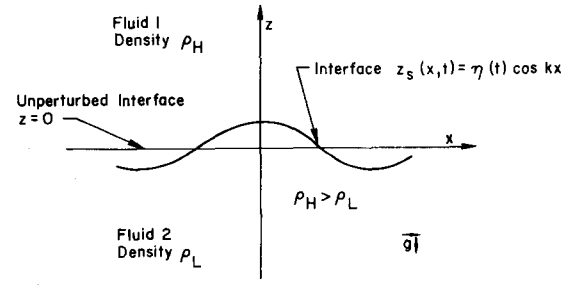

Fig. 3. Two incompressible fluids of infinite depth, having densities ρ_H, ρ_L, meet at an interface. For $t < 0$, the interface is the plane $z = 0$. For times $t \geq 0$, the interface has a perturbed shape. The simple case $Z_s = \eta(t) \cos kx$ is illustrated in the figure.

This is the picture for $t < 0$. At $t = 0$, we perturb the configuration in some way. We might suppose that the fluid is initially at rest but that the interface is perturbed so as to have the form

$$Z_s = \eta(t) \cos kx, \quad [\eta(t)/\lambda \ll 1]. \tag{1}$$

Thus the interface now consists of a set of crests and troughs parallel to the y-axis.

One may then show, using either a potential theory argument via Bernoulli's equation or a simple energy analysis, that the amplitude of the perturbation is determined by the equation [10]

$$\ddot{\eta}(t) = \alpha^2(k)\eta(t), \tag{2}$$

with

$$\alpha^2(k) = G\left(\frac{\rho_H - \rho_L}{\rho_H + \rho_L}\right)k - \left(\frac{\sigma}{\rho_H + \rho_L}\right)k^3. \tag{3}$$

Here σ is the coefficient of interfacial tension.

The solution to (2) for fluids initially at rest is

$$\eta(t) = \eta(0) \cosh \alpha t. \tag{4}$$

Several simple but useful conclusions can be drawn from (3):

If $\sigma = 0$, $G > 0$ and $\rho_H > \rho_L$, α is real and the interface is unstable. The growth rate for short wavelengths is unbounded, so on the basis of linear analysis the Rayleigh–Taylor problem would appear to be ill-posed in the absence of surface tension. However, we note that there is no rigorous theorem available which says either that the Rayleigh–Taylor problem is ill-posed in the absence of surface tension or that it is well-posed when surface tension is included. For $G < 0$, α is imaginary and one has stable gravity waves.

Surface tension stabilizes perturbations shorter than a critical wavelength

$$\lambda_c = [\sigma/G(\rho_H - \rho_L)]^{1/2}. \tag{5}$$

The shape of the dispersion curve makes it plain (fig. 4) that there is a fastest growing, or most unstable, wavelength λ_M. This is given by

$$\lambda_M = \sqrt{3}\lambda_c. \tag{6}$$

The above analysis can be generalized in several ways. For example, in the linear approximation we can superpose harmonic interface perturbations in the x and y directions to give a three-dimensional treatment of the instability.

Also, the linear treatment can be generalized to include other physical effects such as compressibility [11, 12], nonuniform accelerations [13], shocks [14], density gradients [10, 15], slab geometry [16], and so forth. A thorough analysis of the role of viscosity is available [10, 17, 18].

Finally, one can treat general initial conditions [18, 19]. Solutions of the linearlized equations satisfying general initial conditions can be expressed in terms of Fourier–Laplace transforms of the hydrodynamic variables, although the results can get quite complicated.

7.1.2. *Spherical geometry*

Taylor instability at a spherical interface has been studied by several authors [20–25]. Results of generality comparable to those obtained in plane geometry are not available, owing to the greater mathematical complexity of the equations encountered in curved geometries. There is, moreover, a new effect at work in curved geometries – a convergent geometry can itself be destabilizing.

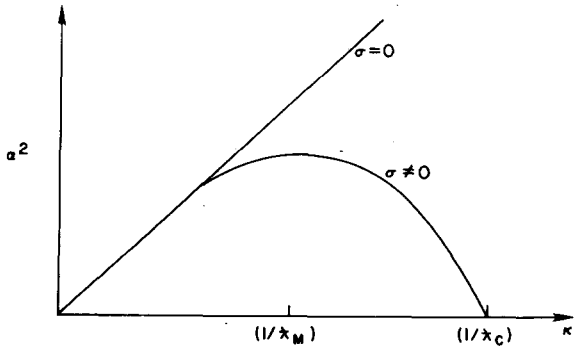

Fig. 4. Schematic plot of α^2 vs. k, eqn (3).

This can be seen readily in the case where the fluids are incompressible [25]. If $R(t)$ is the radius of the unperturbed spherical interface, and if the perturbations δR are expanded in Legendre functions, $\delta R = \Sigma_n a_n(t) P_n(\cos\phi)$, then the amplitudes $a_n(t)$ can be shown to satisfy

$$\ddot{a}_n(t) + (3\dot{R}/R)\dot{a}_n(t) - \alpha^2(n)(\ddot{R}/R)a_n(t) = 0\,, \qquad (7)$$

with

$$\alpha^2(n) = \frac{n(n-1)\rho_2 - (n+1)(n+2)\rho_1}{n\rho_2 + (n+1)\rho_1}\,. \qquad (8)$$

Here ρ_2 = the density outside the interface, ρ_1 = the density inside the interface, and n = the mode number of the spherical harmonic describing the perturbation.

For large R, (7) goes over to the usual Rayleigh–Taylor result. However, if $\rho_1 \to \rho_2$, (7) takes the form

$$\ddot{a}_n(t) + (3\dot{R}/R)\dot{a}_n(t) + (2\ddot{R}/R)a_n(t) = 0\,. \qquad (9)$$

This equation can have unstable solutions, depending on the behavior of $R(t)$. Thus a spherical interface can be unstable even if there is no discontinuity in density across it. The relative importance of classical Rayleigh–Taylor effects and geometric or convergence effects depends strongly on compressibility and the acceleration history of the interface. This dependence can best be studied numerically.

7.2. *Nonlinear modeling*

Next I will briefly discuss some attempts to model the nonlinear growth of spikes and bubbles.

First, an exact closed form solution valid for a finite time T has been derived by Ott [26] for the Taylor unstable motion of a fluid layer idealized as having infinitesimal thickness. An initial sinusoidal perturbation evolves into a cycloid. After time T adjacent segments of the fluid collide and the development cannot be followed analytically.

There have been a number of attempts to model the growth of spikes and bubbles in more general settings. These models are based on one or another set of drastic simplifying assumptions which it is hoped capture the zeroth order physics correctly and permit the dynamics to be described by ordinary differential equations.

The easiest model to describe is that of Fermi [27], who considered incompressible fluids in the limit of infinite density ratio. He considered an initial sinusoidal perturbation, which was then approximated by a polygon, i.e., by a square wave profile (fig. 5). The interface is thus described by 3 parameters; the heights of the spike and bubble (a, b), and the width of the spike (x). The condition of incompressibility provides one relation between these parameters. Fermi next estimates the kinetic energies associated with the horizontal and vertical motions of the spike, and with the motion of the fluid above the spike and bubble, as well as the potential energy of the fluid, in terms of the parameters a and x. This yields a set of coupled nonlinear ordinary differential equations for $a(t)$ and $x(t)$. The results were that the asymptotic speed of the spike was roughly correct, but the speed of the bubble was not correct.

More recent attempts along these lines are due to Baker and Freeman [28] and Crowley and Levermore [29]. Baker and Freeman [28] derive (uncoupled) ODE's for the time evolution of spike

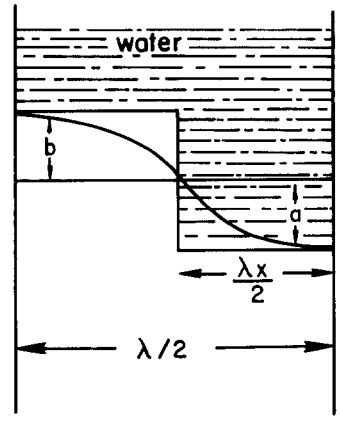

Fig. 5. Fluid configuration analyzed in Fermi's model.

and bubble peak amplitudes by devising functions which interpolate regimes of small and large amplitude behavior. The model produces results for the motion of the tips of spikes and bubbles which appear to be in reasonable agreement with code and experimental determination of these quantities.

Crowley and Levermore [29] have devised an ODE for the time development of an amplitude which is in some sense an envelope of an ensemble of initial perturbations.

My appraisal of this kind of work is as follows:

If such models should turn out to be sufficiently accurate for their intended application, they would enjoy the advantage of any good model: They would express in relatively simple form the governing physics of the problem.

It is not possible to assess a priori the validity of the approximations made in deriving the models. This means that they must be developed in close conjunction with numerical codes and, where possible, experiment. This is no bad thing – indeed, one would hope that high quality codes might help one to develop more refined and better validated models.

A weak point of such models is that they do not seem to help with the most difficult aspects of Rayleigh–Taylor instability: interactions of perturbations of different frequency, the effects of statistically distributed heterogeneities, break-up of spikes and bubble amalgamation.

7.3 *Rising bubbles*

There are a number of studies which analyze the motion of symmetrical bubbles rising under gravity. The steady state motion of cylindrically symmetric bubbles rising in a tube of circular cross section has been treated by Davies and Taylor [30], who give approximate expressions for the speed of the tip of the bubble and for the profile of the bubble near the tip. Layzer [31] has given an approximate solution to the nonlinear equations determining this flow which interpolates between the initial small amplitude motion and the steady state motion.

Birkhoff and Carter [32] and Garabedian [33] discuss plane bubbles rising between parallel walls. They formulate this problem rigorously in terms of nonlinear integral equations, and their work includes an investigation of the existence and uniqueness of solutions to these equations.

Although bubble rise in a gravitational field is not identical to the Rayleigh–Taylor problem, it is closely related and is of course of interest in its own right. Moreover, the results of Davies and Taylor and of Layzer have been incorporated into certain phenomenological models of the late stage of Taylor instability, while those of Birkhoff and Carter have proven useful in validating numerical codes which compute Taylor instability. Also, the papers of Birkhoff and Carter and of Garabedian are examples of a rather sparse body of mathematically rigorous work on problems closely related to Taylor instability.

8. Numerical computation

In the simplest formulation of Rayleigh–Taylor instability, the governing equations are the two-fluid, two-dimensional incompressible Euler equations. As mentioned above, these equations appear to be ill-posed in that the growth rate of short wavelength perturbations is unbounded. We have also pointed to many factors which can influence the development of Taylor instability. These result in modifications to the simple form of the Euler equations, possibly so as to render them well-posed. However, in many cases of physical interest, the extra physical factors occur multiplied by a small parameter. In others words, they occur on small length scales, inaccessible to feasible calculations.

There are two obstacles to correct calculation in such circumstances. The small parameter, small length scale effects must somehow be included by mathematical or computational modeling. At the same time, it is necessary to avoid the incorrect simulation of physical effects by numerical artifacts. In particular convergence under mesh

refinement, while a necessary aspect of validation for such problems, is not sufficient. Validation requires quantitative agreement with an independently correct calculation, analytic solution or laboratory experiment.

The computational strategies which have been developed for this problem fall into the two classes: special purpose codes and general purpose codes. The special purpose codes are ones not readily adaptable to include the variety of physical factors mentioned above. This narrower scope permits analytic simplifications which are utilized to a maximum degree.

Two notable examples of such codes have been developed by Menikoff and Zemach [34, 35] and by Baker, Meiron, and Orszag [36]. The Menikoff–Zemach code is based on conformal mappings. In the case of an infinite density ratio and two fluids in an infinite strip, a time dependent conformal mapping takes the region occupied by the heavy fluid into an infinite half strip. In this half strip, the known Green's function for Laplace's equation is used to express the interface velocity as a quadrature. The code of Baker et al. [36] is based on boundary integral techniques, in which the velocity potential is expressed as an integral over a dipole sheet distributed over the fluid interface. Coupled Fredholm integral equations can then be derived which determine the strength of the dipole sheet, and its time development.

The strong points of the special purpose codes are accuracy and speed. Thus they can be used to validate general purpose codes. Of course, these codes have also been applied in their own right to study several interesting questions. For example, the code of Baker et al. [36] has been used to study Taylor instability of a thin fluid layer [37] (fig. 6), and both codes have been used to confirm results on rising plane bubbles originally obtained by Birkhoff and Carter [32].

There have been numerous calculations of Rayleigh–Taylor instability using codes which solve the full (two-dimensional) Euler or Navier–Stokes equations. Notable examples include the work of F. Harlow and J. Welch [38], B.J. Daly [39, 40], W.P. Crowley [29], J.R. Freeman, M.J. Clauser and S.L. Thompson [41], K.A. Meyer and P. J. Blewett [42, 43] as well as the work cited in refs. 5 and 37.

Time does not permit a systematic review of this work, nor would it be easy to carry out such a review, even if time were not a constraint, because the published work often lacks the detail necessary to evaluate just what is done.

I will instead merely summarize a few of my general impressions:

The codes run up to an aspect ratio of ≈ 1 or 2,

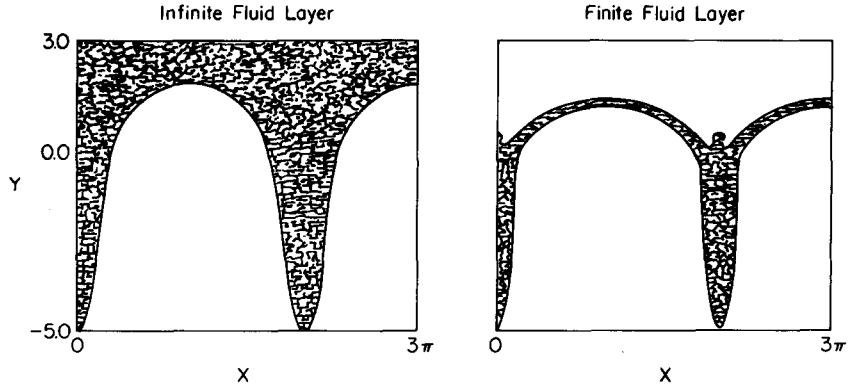

Fig. 6. Plot of interfaces for Rayleigh–Taylor instability of layered flow of an ideal fluid. The Atwood number is unity. Left: Case of a semi-infinite fluid. Right: A finite fluid layer. Figure is adapted from Verdon et al., ref. 37.

where they break down for reasons that are often not thoroughly understood.

The codes have been used to study the effect of factors such as the Atwood number, surface tension, viscosity, compressibility, thermal conductivity and others on the development of the instability. The case of single frequency perturbations is the one commonly treated;

The results are often compared to those of the linear theory. In general, they lack sufficient validation in the nonlinear regime. This is a situation which could be improved substantially if cross comparisons of general purpose codes were more common and more precise.

I now want to turn briefly to a code which I have been working on with Glimm, McBryan, and Menikoff [44]. It is based on the method of front tracking, whose goal is to achieve the accuracy of a special purpose calculation within the context of a general purpose method. The main idea of front tracking is to introduce as a computational degree of freedom an interface consisting of a (codimension one) set of curves, composed for example of piecewise linear bonds joining vertices. The front is propogated using the velocity or acceleration fields of the fluid in the case of a fluid interface discontinuity. Thus, in the Rayleigh–Taylor problem front tracking is a mixed Euler–Lagrange approach, with the front being a Lagrangian degree of freedom and all other grid points being Eulerian. In the incompressible case, it is necessary to solve elliptic PDE's at each time step for the pressure and stream function. The density discontinuity leads to elliptic equations which are singular exactly on the interface, either in their coefficients or their source terms or both.

I will not go into the computational strategies we employ to deal with these problems, or into the structure of the code and related computer science questions, or into a discussion of our current results since these points will be covered in McBryan's talk [45].

I would like to emphasize that in most cases of practical interest, one does not know in detail the nature of the many disturbances perturbing the fluid motion. In general, statistically distributed heterogeneities on various length scales will be present in the driving forces, the velocity fields and in other physical quantities. In some cases, these heterogeneities can strongly influence the fluid motion. Thus, an adequate treatment of Rayleigh–Taylor instability will require analysis not only of the growth of perturbations of fixed wavelength, but of statistical perturbations as well.

The input to our code presently allows one to add a statistically distributed component on one or several length scales to the x and y components of the velocity or acceleration, to the vorticity in the interior of the fluid, and to other physical quantities [44]. This is done by using a random number generator to define a randomly distributed variable on a lattice of points in the (x, y)-plane. The computed functions are modified at each time step by the addition of a random function.

There are many points which need to be studied in connection with statistical perturbations. First, there are now two competing effects at work: heterogeneity and nonlinear growth of fixed perturbations. Introduction of heterogeneity directly affects the physics. The driving forces associated with heterogeneity may set a length scale of their own for the formation of bubbles and spikes. These will compete with and modify the development of deterministically specified perturbations, which are channeled into their own length scales by the nonlinear dynamics.

These points are illustrated in figs. 7–12. Fig. 7 shows the growth of a small amplitude, fixed wavelength perturbation at an air–water interface (density ratio $\approx$ 500:1). In fig. 8, we show how the results in fig. 7 are modified when a strong statistical heterogeneity is added to the vorticity in the interior of the fluids. In particular, two spikes are present now where there was one before. The velocity fields are displayed in figs. 9 and 10, to show the nature of the vorticity which has been added.

In fig. 11, we show the evolution of a larger amplitude, fixed wavelength perturbation at an interface between fluids having a 4:1 density ratio.

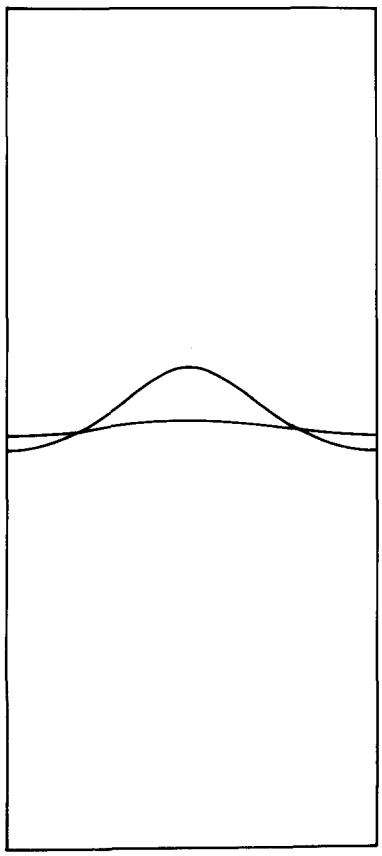

Fig. 7. Nonlinear growth of a fixed wavelength, small amplitude perturbation. In this run the density ratio was $\rho_H/\rho_L \approx 500$, the initial implitude (in units of wave number × amplitude) was 0.1, and the grid size was 48 × 48.

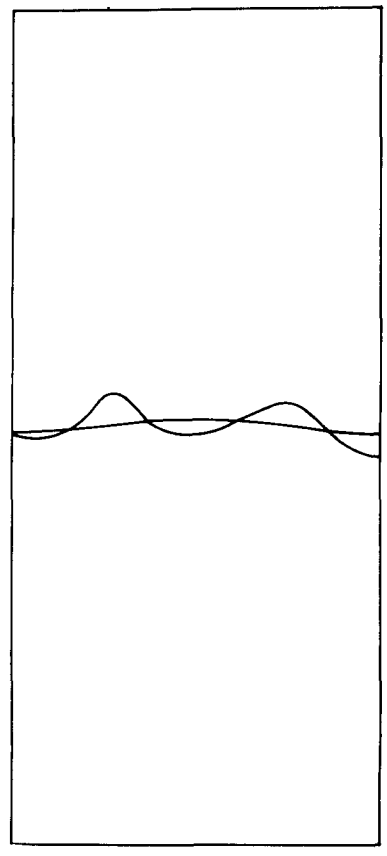

Fig. 8. Growth of a fixed wavelength, small amplitude perturbation in the presence of strong statistical heterogeneity in the vorticity in the interior of the fluid. Other parameters are as in fig. 7.

Fig. 12 shows the effect of adding a strong statistical heterogeneity to the vorticity in this problem, which is to modify the speed and shape of both bubble and spike.

To obtain useful results, one will have to identify aspects of the nonlinear growth which tend to be independent of the details of how the instability is excited. In other words, we need to seek functionals of the solution which are statistically stable. These will be the quantities on which it is appropriate to base design considerations. It is my hope that our work can be joined to the very interesting results recently obtained by Youngs [46] in the case of statistical perturbations of an interface to learn more about these questions in the near future.

9. The late stage of Rayleigh–Taylor instability

I next want to discuss some issues relating to the very late stage of Rayleigh–Taylor instability, during which processes such as bubble amalgamation, spike break-up, and turbulent mixing occur.

9.1. *Bubble amalgamation*

A very primitive statistical model for the process of bubble amalgamation was proposed quite some time ago by Wheeler and myself [47].

We suppose that after an initial period of linear growth, one may consider the Taylor unstable interface to consist of a collection of bubbles of

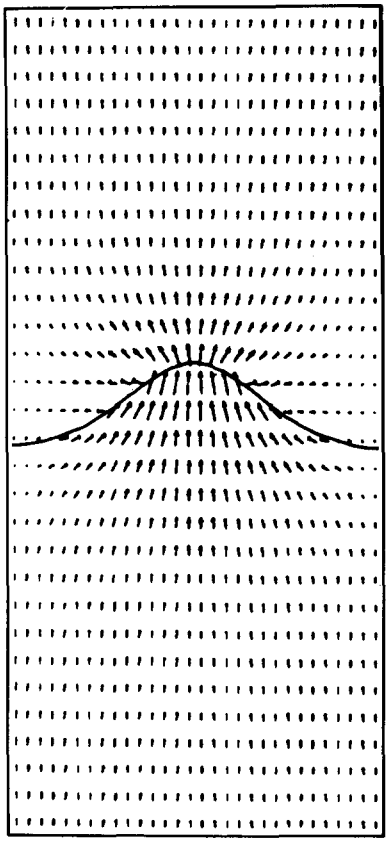

Fig. 9. This figure shows the velocity field associated with the interface motion displayed in fig. 7.

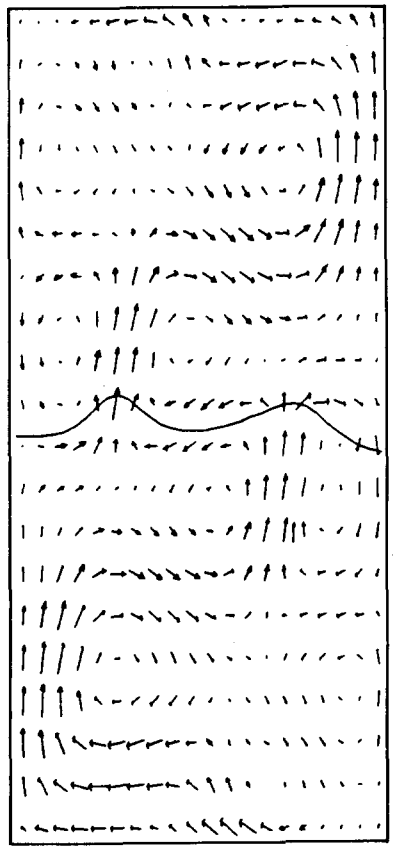

Fig. 10. This figure shows the velocity field associated with the interface motion displayed in fig. 8.

light fluid rising through a slab of heavy fluid. The cross-sectional area of the ith bubble is assumed to be circular, of radius R_i, so that it rises with a velocity given by the Davies–Taylor formula [30]

$$v_i \approx \tfrac{1}{2}\sqrt{gR_i}\,. \tag{10}$$

We also suppose that the sizes of the bubbles are not all the same, but are statistically distributed about an average size R_{av}. As a result, the bubbles will move at different rates and, in particular, a large bubble will move ahead of a smaller neighbor. The experimental evidence suggests that two such neighboring bubbles will merge, forming a single larger bubble.

Our first step was to write down a simple but crude set of rules governing bubble merger. These were:

Rule # 1. Two contiguous bubbles merge when;

$$z_+ - z_- \geqslant R_-\,. \tag{11}$$

Here $z_{+(-)}$ = (volume of bubble)/(cross sectional area of bubble) = effective height of large (small) bubble, R_- = radius of smaller bubble. This rule expresses the idea that the lead of the larger bubble over the smaller bubble necessary for merger will increase as the fraction R_-/R_+ increases.

Rule #2. Conservation of cross-sectional area;

$$\pi R_m^2 = \pi R_+^2 + \pi R_-^2\,. \tag{12}$$

This rule provides a way to calculate the radius of the merged bubble.

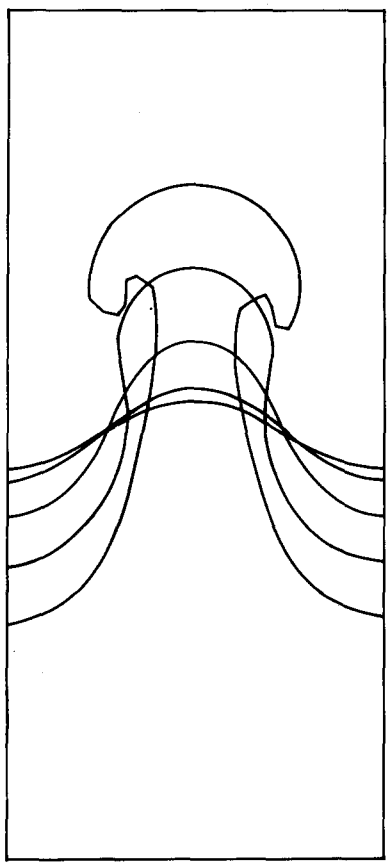

Fig. 11. Nonlinear growth of a fixed wavelength perturbation. In this run the density ratio was $\rho_H/\rho_L = 4$, the initial amplitude (in units of wave number × amplitude) was 0.5, and the grid size was 20 × 20.

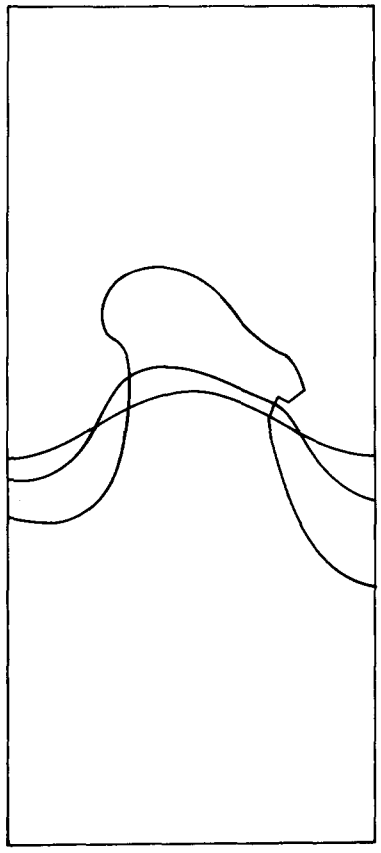

Fig. 12. Growth of a fixed wavelength perturbation in the presence of strong statistical heterogeneity in the vorticity in the interior of the fluid. Other physical parameters are as in fig. 11, except that the grid size here was 40 × 40.

Rule # 3. Conservation of volume;

$$\pi R_m^2 z_m = \pi R_+^2 z_+ + \pi R_-^2 z_- . \tag{13}$$

This rule provides a way to calculate the height of the merged bubble.

Thus as initial conditions one gives a statistically distributed set of values R_i and z_i for the collection of bubbles, and the connectivity of the bubble diagram. One can then follow the process of bubble amalgamation, generation by generation.

Analysis of the model has led to two main results:

(i) Since smaller bubbles get continually absorbed into larger ones, and the opposite process of break-up of large bubbles into small ones seems not to occur, the average size of the bubbles, and hence the average velocity of bubble rise, increases with time.

Numerically, we found

$$v_{av} = k_1 g t, \quad k_1 \approx \frac{1}{20} \text{ to } \frac{1}{100}, \tag{14}$$

where g is the bulk acceleration of the slab of fluid. This leads to a simple prediction. The slab will travel a distance $x = \frac{1}{2}gt^2$ in time t. In this time, the bubble will advance a distance $\delta = \frac{1}{2}(k_1 g)t^2$ into the slab. The bubble breaks through a slab of thickness H when $\delta = H$. Hence the slab can only travel a

distance $L = (g/k_1 g)H$ before breakup, i.e., a slab can only be pushed a distance 20–100 times its thickness.

(ii) A second prediction is that a bubble anomalously larger than average will eventually grow to the point where a single large bubble will dominate the flow, provided the slab is thick enough for the merger process to go to completion before breakthrough. It does not seem to me that available computational and experimental information suffice to distinguish between the following possibilities:

(a) one bubble always quickly runs away;

(b) depending on the degree of anomaly in the original distribution of sizes, either one bubble runs away, *or* a standard, stable statistical distribution in sizes is attained, with a corresponding standard law of growth;

(c) a standard distribution of size and rate of rise is almost always reached.

Nor does available information suffice to validate the rules of bubble merger which we have adopted.

9.2. *Break-up of spikes*

At this time, little can be said with confidence about the details of the processes whereby Rayleigh–Taylor spikes break up – into droplets or otherwise. In particular, droplet formation is a three-dimensional effect which occurs on a small length scale, and as such is likely to fall outside the scope of numerical computation for some time. Available experiments on Taylor instability are inadequate as a guide for modeling these effects.

An objective in modeling spike break-up would be to derive semi-empirical formulae, valid in specified parameter ranges, for the spectra of droplet sizes and velocities. This information could then provide the input for models of entrainment, transport, and mixing.

In thinking about these questions, it may be helpful to regard the heavy falling spike as being somewhat analogous to a liquid jet, with the hope that some of the ideas that have been developed to analyze the stability and atomization of jets can be adapted to spikes.

There are a variety of mechanisms leading to jet disintegration [48, 49]. One of the first studies was by Rayleigh [50], who showed that an idealized cylindrical jet is unstable to varicose perturbations if $L > \pi D$ (L = length of the jet, D = jet diameter). This analysis ceases to apply if the jet is too thick or moves too fast, or if surface tension is negligible.

Kevin–Helmholtz instability on the side of a jet is a frequent cause of jet break-up. In this case, the nonlinear phase of Kelvin–Helmholtz instability results in the formation of a turbulent mixing zone, which spreads into the jet. The size and shape of the mixing zone depends on the shape of the nozzle, the presence of turbulence and other factors.

The formation of a mixing zone in the case of plane two-dimensional Taylor instability has recently been studied by Youngs [46, 51]. A very interesting, very important step has been taken towards understanding the mixing zone approach to spike break-up. I am glad Youngs was able to describe his work at this conference [52], because I do not have time to do it justice in this talk.

Numerous patterns of drop sizes and velocities are observed to occur in the atomization regime of jet disintegration [48, 53, 54]. Factors affecting the character of these patterns include surface tension, viscosity and the nature of "aerodynamic" forces that may be present. The variability of the observed patterns also bespeaks the frequent presence of statistical heterogeneities. Hence in the engineering literature one finds several different drop size distributions used to correlate data. For example, one distribution for the probability $p(d)$ for a drop to have a diameter between d and $d + \delta d$ is the Nukiyama–Tanasawa law [54]

$$p(d) = Ad^m \mathrm{e}^{-bd^n}, \tag{15}$$

where A, b, m, and n are parameters. This law is interesting in that its general form can be derived from statistical considerations together with simple

(but not necessarily correct!) assumptions about droplet formation.

10. The need for experiments

I believe that to carry out informative experiments on the late stage of Rayleigh–Taylor instability is as difficult a challenge for the experimenter as the calcuation of this phase of the instability is for the theoretician.

The classic experiments on Rayleigh–Taylor instability are those of Lewis [8] and Allred and Blount [55]. Additional experiments have been carried out by Duff, Harlow and Hirt [56], Emmons, Chang and Watson [57], Ratafia [58], Cole and Tankin [59], Popil and Curzon [60], Read and Youngs [51], and J.F. Barnes et al. [61, 62].

The available experiments are adequate to confirm semi-quantitatively, or perhaps even quantitatively, several predictions of the linear analysis for the initial growth of the instability. The experiments also provide pictures of the development of bubbles and spikes and the work of Ratafia [58] shows Kelvin–Helmholtz roll-up on the spike. Furthermore, the work of Lewis [8], Allred and Blount [58] and Read and Youngs [51] provides some information on bubble amalgamation.

There is a clear need for more and better experiments. First, available experiments are still inadequate for modeling the very late stage of Taylor instability, although the recent experiments of Read and Youngs [51] provide interesting new information on the mixing zone question. Second, experiments are needed to benchmark codes which compute Rayleigh–Taylor instability in circumstances where accurate special purpose codes do not exist for comparison.

To be of most use, the experiments should be designed with two criteria in mind:

They should be analyzable to produce quantitative data on the time history of the unstable interface. The quantitative data may well refer to appropriately chosen statistical quantities rather than to the detailed properties of a specific interface.

The experiments should be performed in an environment where the equation of state of the fluids can be regarded as known. Compounding an analysis of fluid dynamics with uncertainties about material properties will result in confusion about both.

11. Summary – critical issues

I will close by summarizing what I consider to be some critical issues concerning Rayleigh–Taylor instability.

First, it is very important to carry out three-dimensional calculations of Taylor instability [63]. There are several reasons for this: (a) Several features of Rayleigh–Taylor instability are intrinsically three-dimensional, e.g., bubble merger, processes leading to the break-up of spikes, and turbulent mixing; (b) Experiments are likely to pertain to three-dimensional flows; (c) There may be some surprises.

Second, it is important to assess the role of statistically distributed heterogeneities on the growth of the instability. Such heterogeneties will frequently be present in practical situations, and in some cases can modify the flow substantially.

As a final remark, I think it is interesting to ask whether geometric structures having fractal properties can be helpful in understanding a possible chaotic limit of Taylor instability [64].

The background for this idea is roughly as follows. It has been suggested [65] that in fully developed three-dimensional turbulence, in the limit as the Reynolds number approaches infinity, geometric structures are formed having the properties of fractal sets. The formation of objects on smaller and smaller length scales is believed to be the result of repeated generations of Kelvin–Helmholtz instability. The new idea is that the eddies formed in this way may not be space-filling. One consequence of this picture is so-called intermittancy in turbulence; another is correc-

tions to the self-similar behavior described by Kolmogorov's Law.

We believe that a Taylor unstable interface is also subject to Kelvin–Helmholtz instability. Particularly in the case where surface tension is negligible, could successive generations of Kelvin–Helmholtz instability, possibly initiated by small scale heterogeneities, lead to a fractalized interface evolving in a self-similar manner? What would be some observable consequences of this behavior?

Acknowledgments

The author would like to thank J. Glimm, D. Holm, O. McBryan, R. Menikoff, R. Mjolsness, and H. Rose for helpful advice on the preparation of this article.

References

[1] Lord Rayleigh, Scientific Papers, Vol. II (Cambridge Univ. Press, Cambridge, England, 1900), p. 200.
[2] G.I. Taylor, Proc. R. Soc. London Ser. A 201 (1950) 192.
[3] L. Smarr, J.R. Wilson, R.T. Barton and R.L. Bowers, Ap. J. 246 (1981) 515.
[4] M.L. Norman, L. Smarr, J.R. Wilson and M.D. Smith, Ap. J. 247 (1981) 52.
[5] Taylor instability of laser driven fusion targets has been the subject of numerous papers. Some examples are: J.D. Lindl and W.C. Mead, Phys. Rev. Lett. 34 (1975) 1273; R.L. McCrory, L. Montierth, R.L. Morse and C.P. Verdon, Phys. Rev. Lett. 46 (1981) 336; R.G. Evans, A.J. Bennett and G.J. Pert, Phys. Rev. Lett. 49 (1982) 1639; M.H. Emery, J.H. Gardner and J.P. Boris, Phys. Rev. Lett. 48 (1982) 677.
[6] R.A. Gerwin and R.C. Malone, Nucl. Fusion 19 (1979) 155.
[7] A more realistic description of the interaction of laser light with the surface of a fusion target is given in D.W. Forslund, "The Importance of Surface Physics in Laser-Plasma Interactions".
[8] D.J. Lewis, Proc. R. Soc. London Ser. A 202 (1950) 81.
[9] G. Birkhoff, "Taylor Instability and Laminar Mixing", Los Alamos National Laboratory report LA-1862 (1955); Appendices A–H issued as report LA-1927 (1956).
[10] S. Chandrasekhar, Hydrodynamic and Hydromagnetic Stability (Oxford Univ. Press, Oxford, 1961), Chap. X.
[11] M. Mitchner and R.K.M. Landshoff, Phys. Fluids 7 (1964) 862.
[12] M.S. Plesset and D-Y. Hsieh, Phys. Fluids 7 (1964) 1099.
[13] G.H. Wolf, Z. Physik 227 (1969) 291.
[14] R.D. Richtmyer, Comm. Pure and Appl. Math. **13** (1960) 297.
[15] R. LeLevier, G.J. Lasher and F. Bjorklund, "Effect of a Density Gradient on Taylor Instability", Lawrence Livermore Laboratory report UCRL-4459 (1955).
[16] J.N. Hunt, Appl. Sci. Res. A 10 (1961) 45.
[17] R. Menikoff, R.C. Mjolsness, D.H. Sharp and C. Zemach, Phys. Fluids 20 (1977) 2000.
[18] R. Menikoff, R.C. Mjolsness, D.H. Sharp, C. Zemach and B.J. Doyle, Phys. Fluids 21 (1978) 1674.
[19] R.A. Axford, "Initial Value Problems of the Rayleigh–Taylor Instability Type", Los Alamos National Laboratory report LA-5378 (1974).
[20] G.I. Bell, "Taylor Instability on Cylinders and Spheres in the Small Amplitude Approximation", Los Alamos National Laboratory report LA-1321 (1951).
[21] G. Birkhoff, Quart. Appl. Math. 12 (1954) 306.
[22] M.S. Plesset, J. Appl. Phys. 25 (1954) 96.
[23] M.S. Plesset and T.P. Mitchell, Quart. Appl. Math. 13 (1956) 419.
[24] G. Birkhoff, Quart. Appl. Math. 13 (1956) 451.
[25] H.N. Fisher, "Instabilities in Converging Compressible Systems", unpublished, Los Alamos (1982).
[26] E. Ott, Phys. Rev. Lett. 29 (1972) 1429.
[27] E. Fermi, "Taylor Instability of an Incompressible Fluid", Document AECU-2979, Part 1 (1951). Also published in *The Collected Papers of Enrico Fermi*, vol. 2, E. Segré, editor-in-chief (Univ. of Chicago, Press, Chicago, 1965), p. 816. The case of finite density ratio was treated by E. Fermi and J. von Neumann, "Taylor Instability at the Boundary of Two Incompressible Liquids", Document AECU-2979, Part 2 (1953). This article is also published in Fermi's collected papers, vol. 2, p. 821.
[28] L. Baker and J.R. Freeman, "Heuristic Model of the Nonlinear Rayleigh–Taylor Instability", Sandia National Laboratories report Sand80-0700J (1980).
[29] W.P. Crowley, "An Empirical Theory for Large Amplitude Rayleigh–Taylor Instability", Lawrence Livermore Laboratory report UCRL-72650 (1970); D. Levermore, private communication, 1983.
[30] R.M. Davies and G.I. Taylor, Proc. R. Soc. London Ser. A 200 (1950) 375.
[31] D. Layzer, Ap. J. 122 (1955) 1.
[32] G. Birkhoff and D. Carter, J. Math. Mech. 6 (1957) 769.
[33] P.R. Garabedian, Proc. R. Soc. London Ser. A 241 (1957) 423.
[34] R. Menikoff and C. Zemach, J. Comp. Phys. 36 (1980) 366.
[35] R. Menikoff and C. Zemach, "Rayleigh–Taylor Instability and the Use of Conformal Maps for Ideal Fluid Flow", J. Comp. Phys., in press, 1983.
[36] G.R. Baker, D.I. Meiron and S.A. Orszag, Phys. Fluids **23** (1980) 1485.
[37] C.P. Verdon, R.L. McCrory, R.L. Morse, G.R. Baker, D.I. Meiron and S.A. Orszag, Phys. Fluids 25 (1982) 1653.
[38] F.H. Harlow and J.E. Welch, Phys. Fluids **9** (1966) 842.
[39] B.J. Daly, Phys. Fluids 10 (1967) 297.

[40] B.J. Daly, Phys. Fluids 12 (1969) 1340.
[41] J.R. Freeman, M.J. Clauser and S.L. Thompson, Nucl. Fusion 17 (1977) 223.
[42] K.A. Meyer and P.J. Blewett, "Some Preliminary Numerical Studies of Taylor Instability which Include Effects of Material Strength", Los Alamos National Laboratory report LA-4754-MS (1971).
[43] K.A. Meyer and P.J. Blewett, Phys. Fluids 15 (1972) 753.
[44] J. Glimm, O. McBryan, R. Menikoff and D.H. Sharp, "Front Tracking Applied to Rayleigh–Taylor Instability", in preparation, 1983.
[45] O. McBryan, "Computing Discontinuous Flows", these proceedings.
[46] D.L. Youngs, private communication, 1983.
[47] D.H. Sharp and J.A. Wheeler, "Late Stage of Rayleigh–Taylor Instability", Institute for Defense Analyses, Unpublished report (1961).
[48] G. Birkhoff and E.H. Zarantonello, Jets, Wakes and Cavities (Academic Press, New York, 1957), chap. XV.
[49] S. Chandrasekhar, ref. 10, chap. XII.
[50] Lord Rayleigh, Scientific Papers, vol. I (Cambridge Univ. Press, Cambridge, England, 1899), p. 361.
[51] K.I. Read and D.L. Youngs, "Experimental Investigation of Turbulent Mixing by Rayleigh–Taylor Instability", AWRE report No. 011/83, (1983).
[52] D.L. Youngs, "Turbulent Mixing by Rayleigh–Taylor Instability", Physica 12D (1984) 32, these Proceedings.
[53] R.D. Reitz and F.V. Bracco, Phys. Fluids 25 (1982) 1730.
[54] G.B. Wallis, One-Dimensional Two-phase Flow (McGraw-Hill, New York, 1969), chap. 12.
[55] J.C. Allred and G.H. Blount, "Experimental Studies of Taylor Instability", Los Alamos National Laboratory report LA-1600 (1953).
[56] R.E. Duff, F.H. Harlow and C.W. Hirt, Phys. Fluids 5 (1962) 417.
[57] H.W. Emmons, C.T. Chang and B.C. Watson, J. Fluid Mech. 7 (1960) 177.
[58] M. Ratafia, Phys. Fluids 16 (1973) 1207.
[59] R.L. Cole and R.S. Tankin, Phys. Fluids 16 (1973) 1810.
[60] R. Popil and F.L. Curzon, Rev. Sci. Instr. 50 (1979) 1291.
[61] J.F. Barnes, P.J. Blewett, R.G. McQueen, K.A. Meyer and D. Venable, J. Appl. Phys. 45 (1974) 727.
[62] J.F. Barnes, D.H. Janney, R.K. London, K.A. Meyer and D.H. Sharp, J. Appl. Phys. 51 (1980) 4678.
[63] Preliminary work on the calculation of three-dimensional Taylor instability is reported in S.A. Orszag, "Generalized Vortex Methods in 3-Dimensional Rayleigh–Taylor Instability", Physica 12D (1984) 19, these Proceedings.
[64] This suggestion was formulated in conversations with J. Glimm and H.A. Rose.
[65] B. Mandelbrot, J. Fluid Mech. 62 (1974) 331.